Figure S1

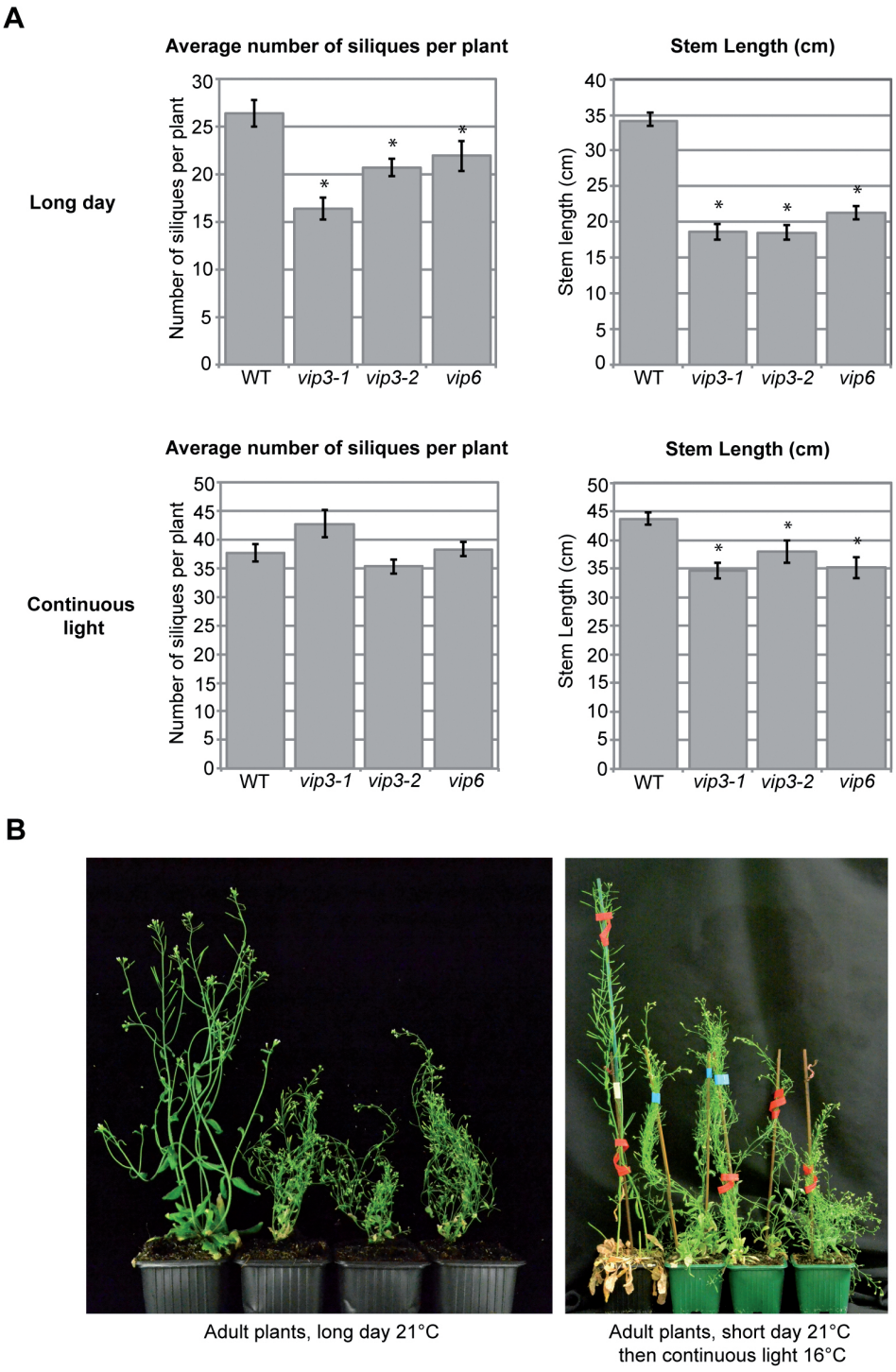

Fig. S1. Effect of growth conditions on *vip* mutant phenotype.

(A) Inflorescence stem length (right) and number of siliques along the main inflorescence stems (left) from plants grown at long day 21°C (referred as "long day") and short day 21°C then continuous light 16°C (referred as "continuous light"). Sample size: number of siliques, long day: WT (n=20), *vip3-1* (n=15), *vip3-2* (n=15), and *vip6* (n=18)); number of silique, continuous light: WT (n=54), *vip3-1* (n=20), *vip3-2* (n=52), and *vip6* (n=30); stem length, long day: WT (n=19), *vip3-1* (n=15), *vip3-2* (n=22), *vip6* (n=14); stem length, continuous light: WT (n=22), *vip3-2* (n=18), *vip3-1* (n=18), *vip6* (n=12). The error bars represent the Standard error of mean, the results were considered significant when $\alpha \leq 0.05\%$ by two-tailed Student tests.
(B) WT and *vip* mutant phenotypes of adult plants grown in long day (left) and continuous light (right) conditions.

Figure S2

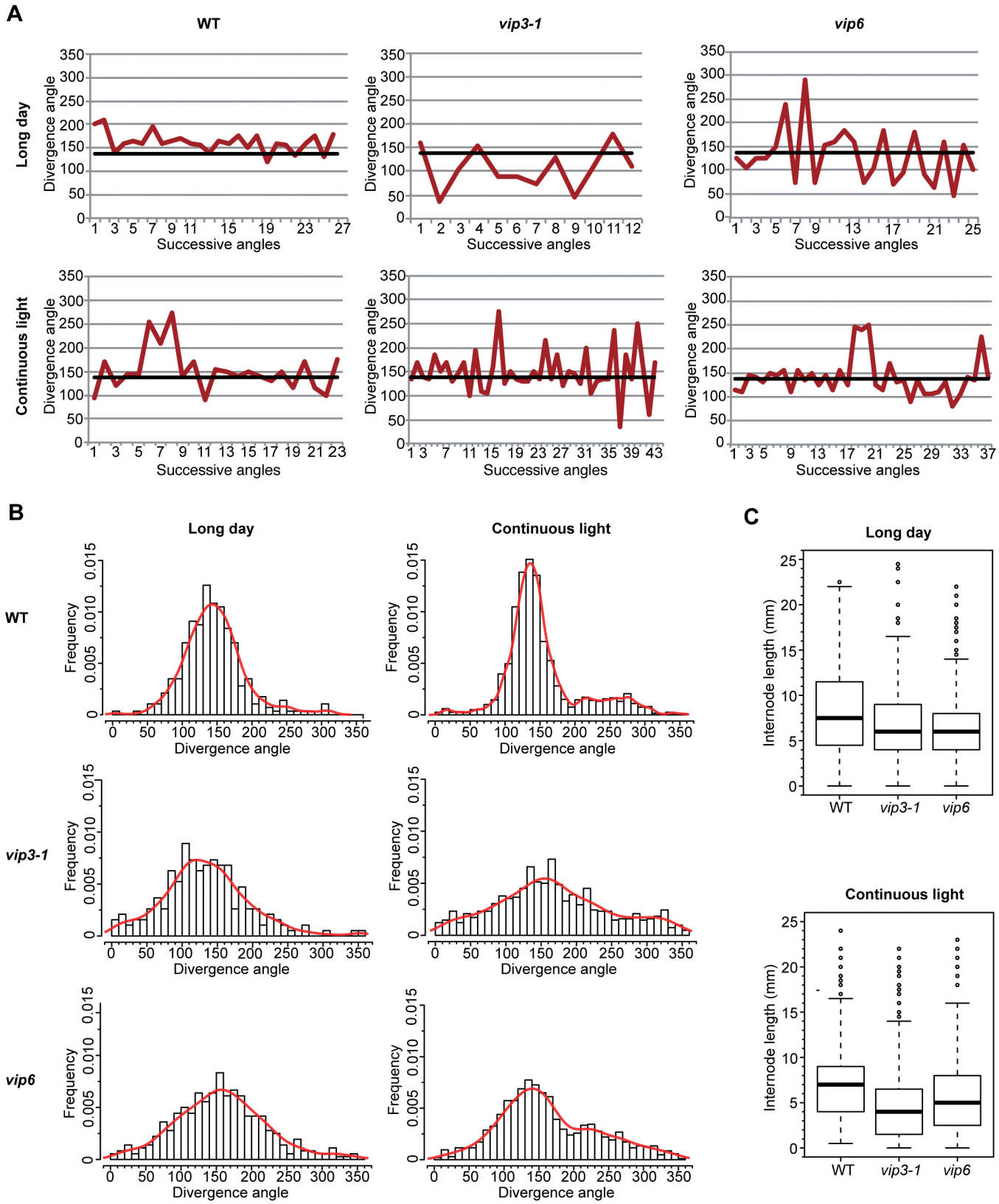

Fig. S2. Phyllotaxis is affected in *vip3* and *vip6* mutant plants.

(A) Sequence of divergence angles in representative WT, *vip3-1* and *vip6* plants grown in long day (upper panel) or continuous light (lower panel) conditions. The thick black line on each graph represents the canonical angle of 137°. (B) Frequency of divergence angles between successive siliques in WT, *vip3-1* and *vip6* plants grown in long day (left panel, WT: 305 angles, 20 plants; *vip3-1*: 201 angle, 15 plants; *vip6*: 366 angles, 18 plants) and continuous light (right panel, WT: 1997 angles, 54 plants, *vip3-1*: 820 angles, 20 plants, *vip6*: 1046 angles, 30 plants) conditions. (C) Average internode length on the inflorescence stem in WT, *vip3-1* and *vip6* plants grown at long day (left panel, WT: 520 internodes, 20 plants; *vip3-1*: 246 internodes, 15 plants; *vip6*: 420 internodes, 18 plants) and continuous light (right panel, WT: 620 internodes, 21 plants; *vip3-1*: 939 internodes, 20 plants; vip6: 1082 internodes, 30 plants) conditions. The black line in the boxplot represents the median, the box represents the distribution range of 50% of the measured values and the bars (whiskers) illustrate the upper and lower quartiles. The average internode length on *vip3* mutant plants is not significantly different from that of the wild type, but the frequency of shorter internodes is increased when compared to wild-type stems

Figure S3

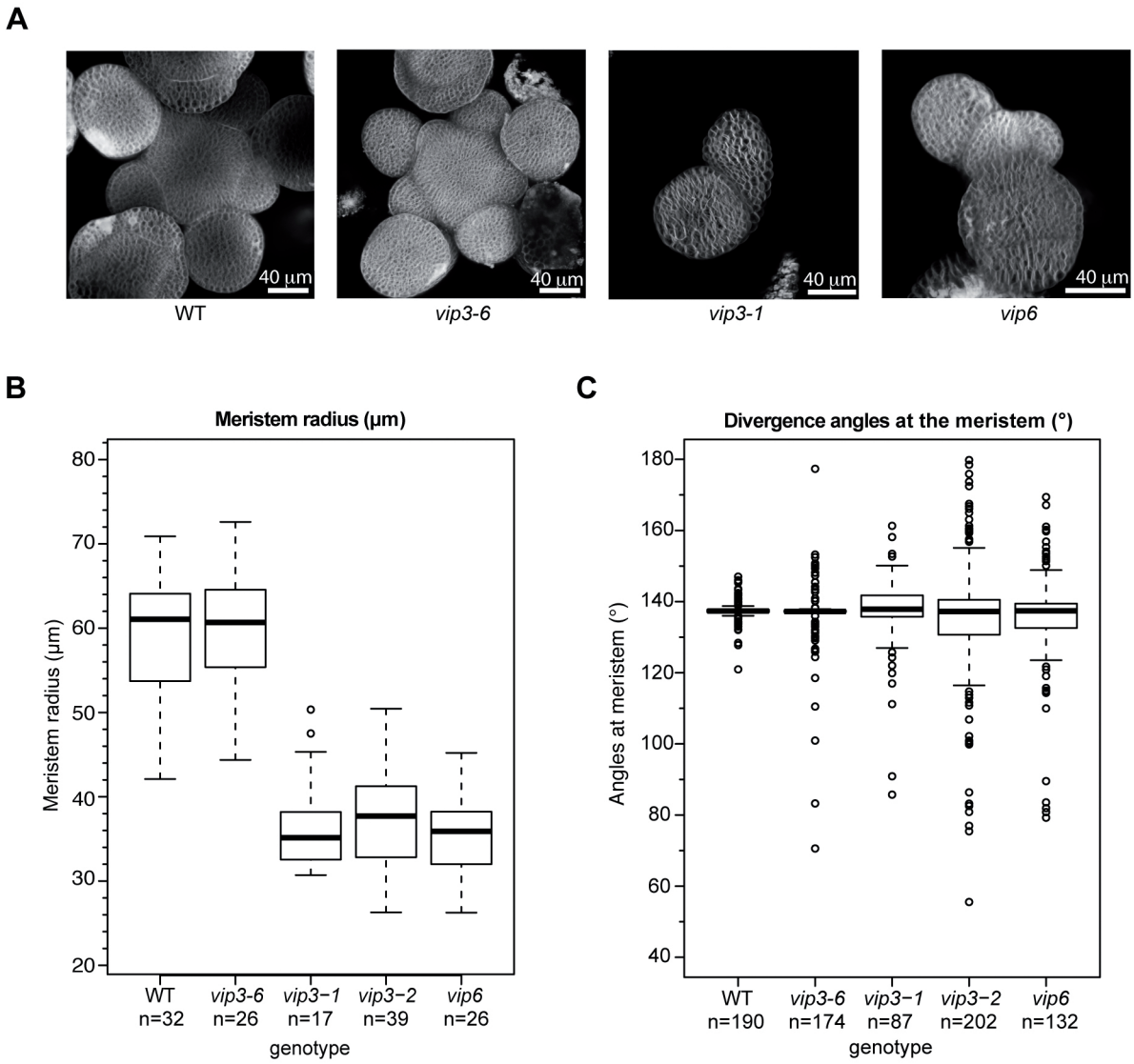

Fig. S3. Meristem size and divergence angles in WT, *vip3-1*, *vip3-6* and *vip6*.

(A) Representative WT, *vip3-6*, *vip3-1*, *vip6* meristems (surface projections), labelled with FM4-64. (B) Meristem radius (µm) in WT (n=32), *vip3-6* (n=26), *vip3-1* (n=17), *vip3-2* (n=39) and *vip6* (n=26) grown in continuous light conditions. Data for the WT and *vip3-2* are reproduced from Figure 4 to ease the comparison between genotypes. Meristem radius was measured as described in (Landrein et al., 2015b) ; α≤0.05% by two-tailed Student tests. (C) Divergence angle between primordia at the SAM in WT (n=190), *vip3-6* (n=172), *vip3-1* (n=87), *vip3-2* (n=202) and *vip6* (n=132). The angles between the successive organs were estimated as described in (Landrein et al., 2015b).

Figure S4

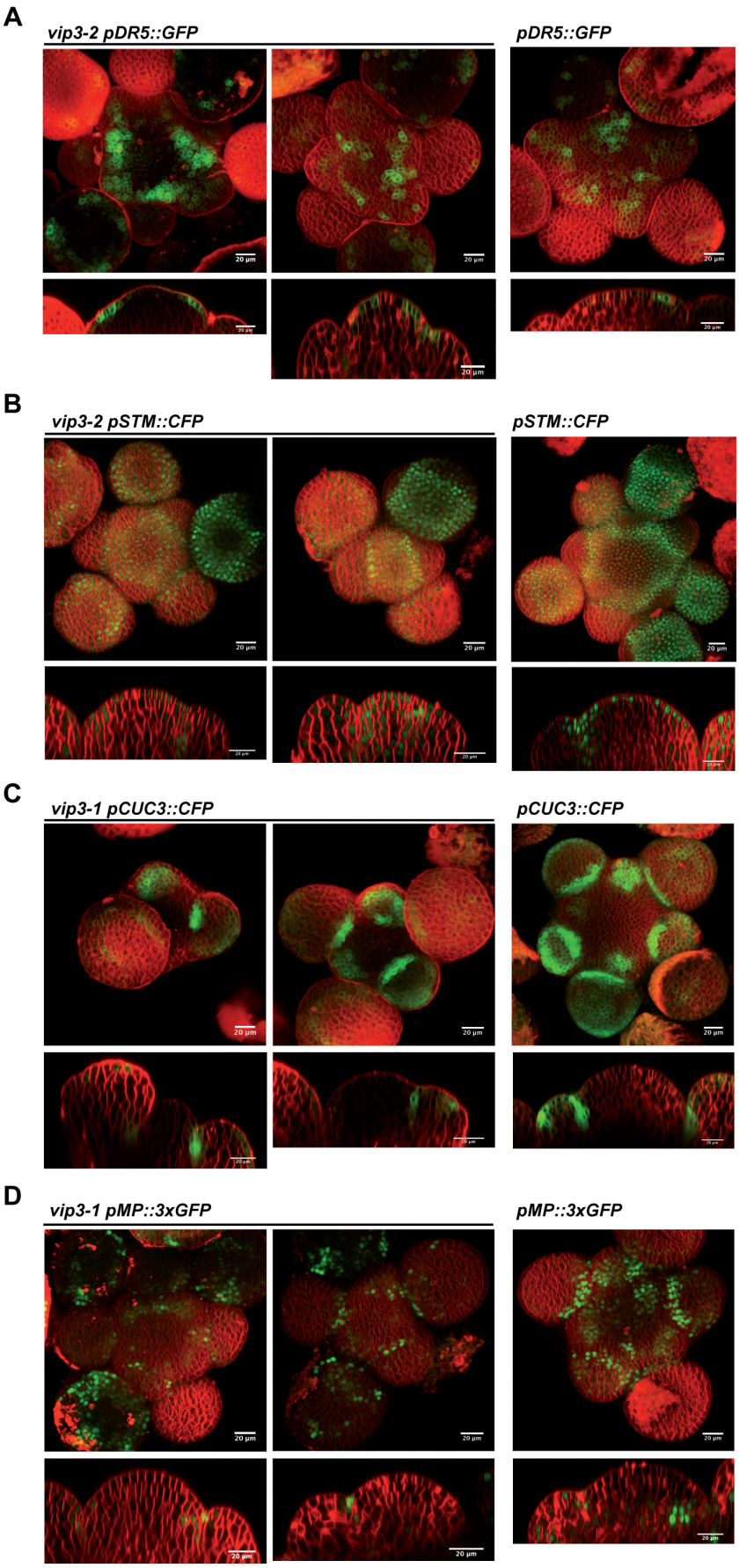

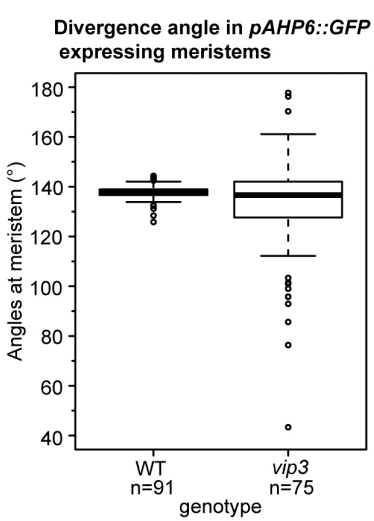

Fig. S4. *pDR5::GFP*, *pSTM::CFP-N7*, *pCUC3::CFP* and *pMP::3xGFP* expression patterns in *vip3*

(A) Two examples of *vip3-2* mutant meristems expressing *pDR5::GFP* (green), labelled with FM4-64 (red). Note the absence of focused DR5 peaks, when compared to the WT (Fig. 5A). Scale bars=20 µm. Lower panels: orthogonal optical sections of the same meristems.
(B) Two examples of *vip3-2* mutant meristems expressing *pSTM::CFP-N7* (green), labelled with FM4-64 (red). Note the stronger expression in boundaries in both WT and mutant. Scale bars=20 µm. Lower panels: orthogonal optical sections of the same meristems.
(C) Two examples of *vip3-1* mutant meristems expressing *pCUC3::CFP* (green), labelled with FM4-64 (red). Note the stronger expression in boundaries in both WT and mutant. Scale bars=20 µm. Lower panels: orthogonal optical sections of the same meristems.
(D) Two examples of *vip3-1* mutant meristems expressing *pMP::3xGFP* (green), labelled with FM4-64 (red). Note the weaker signal intensity when compared to the WT. Scale bars=20 µm. Lower panels: orthogonal optical sections of the same meristems.
(E) Divergence angles between successive primordia in WT (n=91) and *vip3-2* (n=75) mutant meristems with *pAHP6::GFP*. The angles were measured as described in (Landrein et al., 2015b). The boxplots represent the median and the quartile range distribution of the measured values.

Table S1. List of primers

Name	**Sequence**
*VIP3_in_situ*_F	GAGAATGAAACTCGCAGGTC
*VIP3_in_situ*_RT7	TAATACGACT CACTATAGGGCTTGTCATCA GAGACACTAGC
*STM_in_situ*_F	GAGATGTGATCCATTGGGAAAGG
*STM_in_situ*_RT7	TGTAATACGACTCACTATAGGGCGGTCCGATGTGTCCTATGATGATGATG
*CLV3_in_situ*_F	ATGTCCGGTCCAGTTCAACAAC
*CLV3_in_situ*_RT7	TGTAATACGACTCACTATAGGGCGGTCAGGTCCCGAAGGAACA
*MP_in_situ*_F	ATGATGGCTTCATTGTCTTGTG
*MP_in_situ*_RT7	TGTAATACGACTCACTATAGGGCTTATGAAACAGAAGTCTTAA
*GFP_in_situ*_F	AAGAACTTTTCACTGGAGTTGTCCC
*GFP_in_situ*_RT7	TGTAATACGACTCACTATAGGGCCGCTTCCATCTTCAATGTTGTGTCT
LBb1.3	ATTTTGCCGATTTCGGAAC
vip6 F	GATGCAACTGATGGGAAGGACTC
vip6 R	CACCCATACATCAGGCATCTGAAG
vip3-1 F	GACTGCAAGTACCACTTTCGC
vip3-1 R	TAATGGGAAACGACTTGCTTG
vip3-2 F	CTGACTGGATCTCTTGACGAGACG
vip3-2 R	GATACTCAGCAATTCCATATAGTACCCAAGC
vip3-6 F	GCAATTAGCTGACGACGGCGGG
vip3-6 R	GATCCAGCTCGTCCGGTCGCC